



CHARACTERIZATION AND KINETIC STUDIES OF THERMAL DECOMPOSITION OF OBAJANA LIMESTONE USING THERMOGRAVIMETRIC ANALYSIS

Abdul .A, HF Akande and Jibrin .W

Department of Chemical Engineering, College of Industrial Engineering, Kaduna Polytechnic, Kaduna, Kaduna State, Nigeria

Corresponding Author: aadamuabdul@kadunapolytechnic.edu.ng

Abstract

The thermal decomposition of Obajana limestone using Thermogravimetric Analysis (TGA) and Coats-Redfern model was studied with focus on limestone particle size and temperature as process variables of interest. The thermal decomposition was carried inside a TGA where calcium carbonate decomposes to produce calcium oxide and carbon dioxide in the presence of nitrogen. The first order kinetic was used to investigate the thermal decomposition of limestone process by varying the limestone particle size at optimum values of other parameters. Kinetic parameters such as pre-exponential factor (A) and activation energy (E) were then estimated for each of the limestone particle size. The result of the kinetic analysis shows that the most suitable particle size for the first order model is 600 μm producing activation energy of 9.807×10^3 kJ/mol and pre-exponential factor of 8.21×10^9 with coefficient of determination of 0.9957. Also, the values of the kinetic parameters compared favourably with that obtained in literature. The characterization of the Obajana limestone shows that it has the physical, chemical and mineralogical properties of a commercial limestone.

1.0 INTRODUCTION

As it was rightly said by Ar and Dogu (2000), thermal decomposition of limestone has been the subject of intensive study over the years due to its importance in the industry, especially in the flue gas desulphurization and in the hydration of cement industry.

Different models can and have been employed to study the kinetic of limestone calcinations, including heterogeneous model, homogeneous model, intermediate model and power rate law model Sani (2008).

Thermal decomposition (calcinations) of limestone is the process of producing quicklime with the evolution of carbon dioxide (Crain, 2010). Quicklime is one of the world's most useful industrial chemical (Muazu et al., 2011). Also, limestone is ranked as the world's most widely used chemical after petroleum and

occurs in many parts of Nigeria with proven commercial deposits (Muazu et al., 2011) and covering 10% of the earth's land surface and are found in majority of countries (Adedrain et al., 1998).

Therefore, the Kinetic Study of Calcination of the different deposits of limestone across the world cannot be exhausted. There are many reported work on the calcination of kinetics of different limestone but there has not been any on that of Obajana limestone which is abundantly present in Nigeria with proven commercial deposits. It therefore becomes necessary that a fundamental investigation is carried out on Obajana limestone kinetics of calcinations with a view to generate a reliable data for energy saving, product quality, lime kiln design, optimization and modeling and also to provide basis for comparison with other limestone (Adedrain et al., 1998).

Limestone is a sedimentary rock type of solid mineral formed by the accumulation of

sediments in air or water and compose of calcium or magnesium carbonate, Ryemshak et al (2012). The physical and chemical properties of limestone vary widely depending on the route by which they were formed, the sedimentary environment and the changes brought about by diagenesis (i.e. the conversion of sediments into rock by organic physical and chemical processes, Considine (1974). The original material of limestone is calcium carbonate. However, either before or after its consolidation, dissolved magnesium compounds in water may partly replace the calcium with magnesium forming dolomite [CaMg(CO₃)₂]. Thus, limestone may be pure calcite, a mixture of calcite and dolomite or a pure dolomite, Benton (1973).

3.1 Materials and Equipment

3.1.1 Materials

Materials used in this work for the calcination of Obajana limestones are shown in Table 1.

Table 1 Materials and sourced.

| S/NO | MATERIAL | SOURCE |
|------|--------------------|--|
| 1 | Obajana limestone, | Obajana limestone deposits Gombe state |
| 2 | Nitrogen | Solid Mineral Centre kad. Poly kaduna |
| 3 | silica gel | Solid Mineral Centre kad. Poly kaduna |
| 4 | platinum crucible | Solid Mineral Centre kad. Poly kaduna |
| 5 | mortar pestle | Solid Mineral Centre kad. Poly kaduna |
| 6 | lithium bromide | Solid Mineral Centre kad. Poly kaduna |

3.1.2 Equipment

The major equipment used in this research is given in Table 2.

Table 2: Major Equipment Used.

| S/NO | MATERIAL | MODEL |
|------|------------------|----------------|
| 1 | Furnance | Hitachi S-4700 |
| 2 | SEM | Hitachi S-4700 |
| 3 | TGA | STA 6000 |
| 4 | XRF | |
| 5 | Weighing balance | |
| 6 | Diffractionmeter | |

3.1.3 Preparation of Particle Size Samples

The Obajana limestone particles were screened, washed and dried under the sun. The particles were then grinded and sieved with a shaker (tyler mesh) to obtain particle sizes. These particles of different sizes were then heated in a furnace to a temperature of 950°C after which they were placed in a desiccator to cool. Finally, the particles were then weighed with weighing balance to determine the weight loss.

3.2 Methodology

3.2.1 X- Ray Diffraction (XRD)

The prepared sample of a particle size was placed in sample holder of SIEMENS D 500 diffractometer operated at 40kV and 40mA. The attached computer automates the data collection and data reduction steps of the analysis. The divergence slit was set to 1 while the detector slit was set to 0.05. The scanning range (2θ) was performed from 20° to 60° with a step size of 0.02° 2θ .

The computer then scanned the sample and the result was produced.

3.2.2 X-Ray Fluorescence (XRF)

In this work, XRF Phillip MagiX Pro was used, XRF analysis was carried out using the flat lower surface of the disk. The tube voltage of 40 kV and tube current of 30 mA are used to measure the composition of Obajana limestone samples, 0.05g of LiBr was mixed with the sample in the platinum crucible which was transferred to the fusion machine. The fusion machine was programmed for power and fusion time. The fusion machine was started to allow the mixture to melt. The mixture was allowed to cool, solidify and cast.

3.2.3 Scanning Electron Microscope (SEM)

Surface morphology analysis was performed using a Hitachi S-4700 Scanning Electron Microscope (SEM). In a typical test, the Obajana limestone was loaded on a piece of carbon tape located at the top of an

aluminum sample holder. The Obajana limestone was gold-coated using an Emitech 575 Sputter Coater, to eliminate any electron discharges that could reduce the resolution of the sample's image. The Obajana limestone was analysed at 1 Pa with an accelerating voltage of 15kV.

3.2.4 Thermo Gravimetric Analyses (TGA)

The thermo gravimetric Analyses (TGA) was performed with a Model STA 6000, Serial Number: 002041905 and Software Version: 11.0.0.0449. An approximately 30-60 mg sample of Obajana lime stone was loaded in a quartz pan and mounted in the instrument. During the experiments, Obajana limestone samples was heated at 30.0 ml/min in nitrogen at linear heating rates of 10°C/min to 900°C . Under these test conditions, the limestone was held for 1.0 min at 30°C, heated from 30°C to 900°C at 10°C/min and was then held for 5.0 min at

900°C, before being cooled from (900°C) to 30°C at 20°C/min.

3.3 Kinetic Analysis of Non – isothermal TGA Data

Thermal decomposition of limestone was assumed to follow a power law kinetic model. When calcination is performed in the presence of CO₂, the recarbonation of lime also occurs.



3.1

The equation below describes the kinetics of this reversible reaction.

$$\frac{dX_{\text{caco}_3}}{dt} = k_1 S a_{\text{caco}_3} - k_{-1} S a_{\text{cao}} P_{\text{CO}_2}$$

3.2

Where X_{caco_3} is the fraction of CaCO₃ remaining in the sample at reaction time t (minutes), S is the area at reaction interface, a_{caco_3} and a_{cao} are the activities of CaCO₃ and CaO; k_1 and k_{-1} are forward and reverse reaction rate constant (min⁻¹); t , P_{CO_2} (kPa) is the partial pressure of CO₂ in the calcination gas.

X_{caco_3} is defined by equation 3.3 where m_i and m_f are the initial sample mass and final mass at the termination of reaction, m is the mass remaining at reaction time t ; and α is the mass conversion.

$$X_{caco_3} = 1 - \frac{m_i - m}{m_i - m_f} = 1 - \frac{m_i - m}{m_i - m_f} = 1 - \alpha \quad 3.3$$

The activities of solid compounds are assumed to be unity (i.e., a_{caco_3} and $a_{cao}=1$) because the pressure attributed to solid is very small compared to the pressure of gas.

By substituting $k_1/k_{-1} = k_{eq} = P_{CO_2}$ in equation 3.3 and

For $P_{CO_2} \leq P_{CO_2}^*$

Equation 3.4 is obtained. (Craido et al.,

$$1995).- \frac{dX_{caco_3}}{dt} = k_1 S \left(1 - \frac{P_{CO_2}}{P_{CO_2}^*} \right) \quad 3.4$$

In limestone calcination, the reaction interface is not well defined therefore the area of reaction interface is neither easily identified nor can be measured. It can be assumed that $S \propto X_{Caco_3}$ at time t (Campbell

1978). This proportionality is a variable and is expressed as X^{-n} in equation 3.5 below where n is the reaction order with respect to X .

That is

For $P_{CO_2} \leq P_{CO_2}^*$

$$- \frac{dX_{caco_3}}{dt} = k X_{Caco_3}^{-n} \left(1 - \frac{P_{CO_2}}{P_{CO_2}^*} \right)$$

3.5

Substituting equation 3.4 into equation 3.5

would result in equation 3.6 below

$$\frac{d\alpha}{dt} = k(1 - \alpha)^n \left(1 - \frac{P_{CO_2}}{P_{CO_2}^*} \right)$$

3.6

In CO_2 - free environment ($P_{CO_2} = 0$), the calcination reaction involves only the forward reaction of equation 3.6 and reduces to equation 3.7 below;

$$\frac{d\alpha}{dt} = k(1 - \alpha)^n$$

3.7

Equation 3.7 describes thermal decomposition reaction of limestone in absence of mass and heat transfer limitations. Also where $\beta = dT/dt$ is the

constant linear heating rate (k/min) equation

3.7 can be described by the equation below;

$$\frac{d\alpha}{dt} = \frac{d\alpha}{dT} \times \frac{dT}{dt} = \frac{d\alpha}{dT} \times \beta = k(1 - \alpha)^n$$

3.8

Where k is the reaction rate constant which is commonly described by Arrhenius expression.

$$k = A \cdot e^{-\frac{Ea}{RT}}$$

3.9

Where A is the frequency factor (min⁻¹), Ea is the activation energy (kJ/mol), T is the reaction temperature (k) and R is the gas constant (8.316Jmol⁻¹ k⁻¹). Ea, A, and n values are determined from the experimental reaction rate data.

Substituting equation 3.8 into equation 3.9, gives equation 3.10.

$$\frac{d\alpha}{dt} = \frac{A}{\beta} \cdot e^{-\frac{Ea}{RT}} (1 - \alpha)^n$$

3.10

Rearranging and integrating equation 3.10 with boundary conditions $\alpha = 0$ at $T = T_0$ and $\alpha = \alpha$ at $T = T$ to yield 3.11

$$\int_0^\alpha \frac{d\alpha}{dT} \cdot \frac{\beta}{A} \cdot (1 - \alpha)^{-n} = \int_0^T e^{-\frac{Ea}{RT}}$$

3.11

T_0 is the ambient temperature at the beginning of a TGA experiment in most cases. The reaction rate is slow hence it can be ignored (i.e $T_0 = 0$). The RHS of equation 3.11 does not have an exact analytical solution, therefore an alternative equation which gives the approximate solution of this equation is used. (Campbell 1978) That is,

$$\int_0^T e^{-\frac{Ea}{RT}} \cong \frac{RT^2}{Ea} \cdot e^{-\frac{Ea}{RT}}$$

3.12

The kinetic parameters of irreversible calcium carbonate decomposition in a CO_2 – free environment using non – isothermal TGA is determined by integrating and differentiating. This results in, equation 3.13 and equation 3.14 respectively (Campbell, 1978).

$$\alpha = 1 - \left[\left((n - 1) \cdot \frac{ART^2}{\beta Ea} \cdot e^{-\frac{Ea}{RT}} \right) + \right]$$

$$1 \int^{1-n}$$

3.13

$$\frac{d\alpha}{dt} = \frac{A}{\beta} \cdot e^{-\frac{Ea}{RT}} \cdot \left[1 + \left((n-1) \cdot \frac{ART^2}{\beta Ea} \cdot e^{-\frac{Ea}{RT}} + 1 \right)^{\frac{n}{1-n}} \right]$$

$$\frac{d\alpha}{dt} = \frac{A}{\beta} \cdot e^{-\frac{Ea}{RT}} \cdot \left(1 - \frac{P_{CO_2}}{P_{CO_2}^*} \right) \cdot \left[1 + \left((n-1) \cdot \frac{ART^2}{\beta} \cdot \left(\frac{e^{-\frac{Ea}{RT}}}{Ea} - \frac{P_{CO_2} e^{-\frac{Ea-F}{RT}}}{B(Ea-F)} \right) \right)^{\frac{n}{1-n}} \right]$$

3.14

The equilibrium pressure of CO₂, P_{CO_2} in equation 3.14 is replaced by a temperature dependent expression presented in equation 3.15

$$P_{CO_2}^* = B \times e^{-\frac{F}{RT}}$$

3.15

Where B (kPa) and F (kJ/mol) are constants (Campbell, 1978).

The general mathematical expressions describing the thermal decomposition of CaCO₃ in a CO₂ gas environment are represented below.

$$\alpha = 1 - \left[1 + \left((n-1) \cdot \frac{ART^2}{\beta} \cdot \left(\frac{e^{-\frac{Ea}{RT}}}{Ea} - \frac{P_{CO_2} e^{-\frac{Ea-F}{RT}}}{B(Ea-F)} \right) \right)^{\frac{1}{1-n}} \right]$$

3.16

Equation 3.17 predicts the rate of limestone decomposition which decreases with increasing CO₂ partial pressure in the calcination gas at a given reaction temperature. Limestone is thermally decomposed only when the local CO₂ concentration is less than the equilibrium CO₂ partial pressure at a given reaction temperature. Therefore, a higher activation energy and a lower frequency factor are expected when calcination occurs in CO₂.

3.3.1 Determination of Kinetic Parameters

Kinetics parameters for thermal decomposition of limestone samples can be determined by several non-isothermal TGA kinetic analysis methods, e.g, Coats-Redfer (CR), Criado- Linearization, and DTG curve fitting.

3.3.1.1 Coats – Resfern Linearization Technique.

By integrating equation 3.17 for $n = 1$ or $n \neq 1$ and rearranging the equations into their linear forms gives the following equation below

$$\ln \left[\frac{(1-n)^{1-n} - 1}{(n-1)T^2} \right] = \ln \left[\frac{AR}{\beta E_a} \left(1 - \frac{2RT}{E_a} \right) \right] - \frac{E_a}{RT} \quad 3.18$$

$$\ln \left[- \frac{\ln(1-\alpha)}{T^2} \right] = \ln \left[\frac{AR}{\beta E_a} \left(1 - \frac{2RT}{E_a} \right) \right] - \frac{E_a}{RT} \quad 3.19$$

Coats- Redfern method employs equation 3.18 and 3.19 to determine the kinetic parameters in which a reaction order is

initially assumed and the experimental data are plotted, iteration of the values of n is performed until the highest correlation coefficient (R^2) of the plot is obtained. A log-log plot of the left hand side of either equation 3.18 or equation 3.19 against $1/T$ in the major decomposition stage of limestone is then prepared.

The slope and intercept would be calculated using the equations below;

$$\text{Slope} = \frac{E_a}{R} \quad 3.20$$

$$\text{Intercept} = \ln \left[\frac{AR}{\beta E_a} \left(1 - \frac{2RT}{E_a} \right) \right] \quad 3.21$$

From equation 3.20 and equation 3.21, activation energy and frequency factor are calculated. Thus,

$$E_a = \text{slope} \times R \times T \quad 3.22$$

$$A = \frac{\exp(\text{intercept}) \times \beta \times E_a}{R \times \left(1 - 2 \frac{RT}{E_a} \right)} \quad 3.23$$

4.0 RESULTS AND DISCUSSION

4.1 Characterization of Limestone

Samples

In this chapter, the experimental results were given and discussed in the following order;

X-Ray Diffraction (XRD), X-Ray fluorescence (XRF), Scanning Electron Microscope (SEM) and Thermogravimetric Analysis (TGA).

Figure 1: **Experimental Result of X-Ray Diffraction (XRD)**

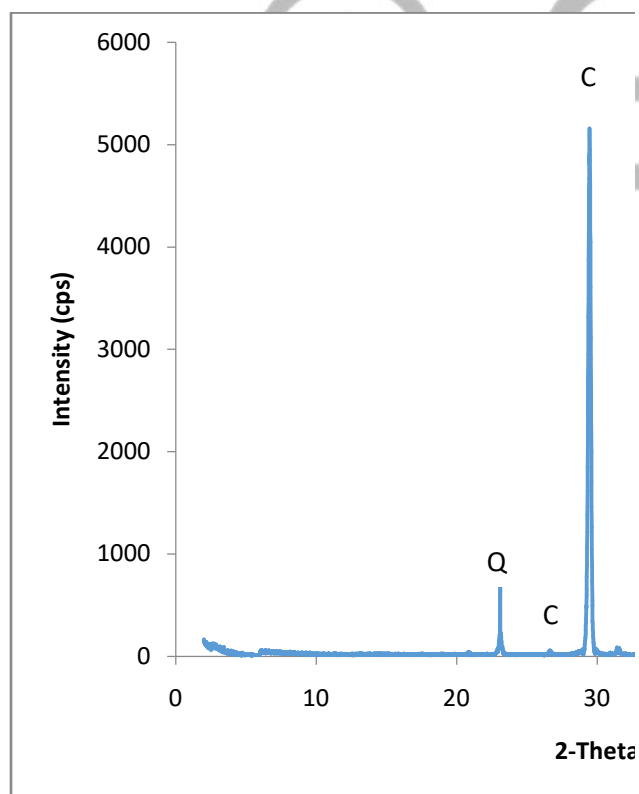


Figure 4.1: XRD Diffraction of Obajana Limestone

The XRD diffractogram of Obajana limestone was carried out using X-ray diffractometer as shown in Figure 1. The diffractogram were matched with ICDD data to determine the mineral phases present in Obajana limestone sample. The peak matching with ICDD data shows that calcite were the mineral phases identified at d-spacing of 29.46°, 20.97°, 36.03°, 39.46°, 43.23°, 47.59°, and 48.59°. 5153, 33, 320, 494, 455, 565, and 426 respectively.

Dolomite and quartz were identified at d-spacing of 42.1° and 23.1° respectively. It

can be in C - Calcite that calcite
 D = Dolomite
 is the pr Q - Quartz (Silica) e identified

in Obajana limestone. This was followed by quartz and dolomite. This result is in agreement with the result obtained in the work of Anbalagan et al. (2009).

C C D C C C
 Figure 2. **Experimental result of**

Scanning Electron Microscope (SEM)

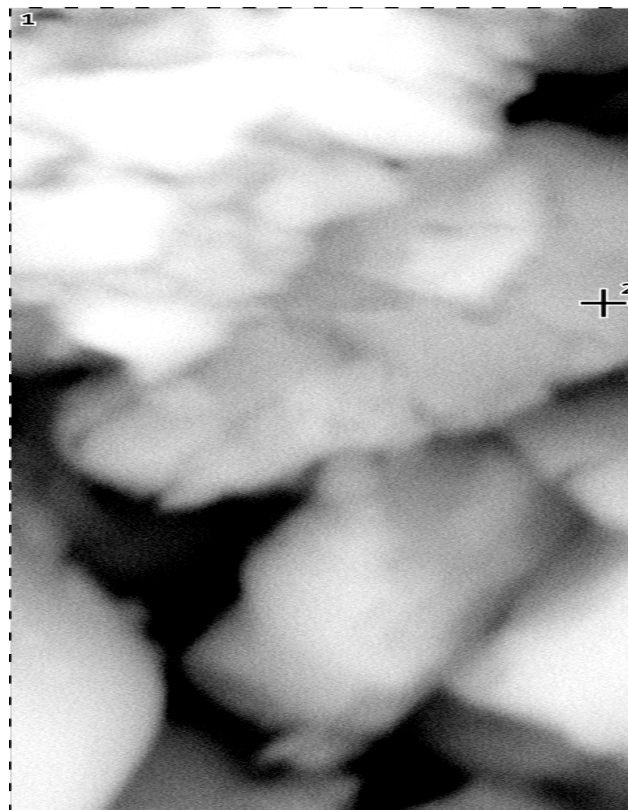


Figure 2: SEM Image of Obajana Cement.

Figure 2 showed that the white pores in the image confirm that Obajana limestone has micritic calcite crystals containing high amounts of calcium oxide.

4.1.3 Experimental result of X-Ray Fluorescence (XRF)

In order to know more about the characterization of Obajana limestone, XRF experiment was carried out, the result is given below:

Table 3: Composition of Elements in Obajana Limestone.

| S/No | Elements | Obajana Limestone (%ppm) |
|--------------|--------------------------------|--------------------------|
| 1 | Al ₂ O ₃ | 0.1777 |
| 2 | CaO | 92.9345 |
| 3 | Cd | 0.0034 |
| 4 | Co | 0.0029 |
| 5 | Cr ₂ O ₃ | 0.00622 |
| 6 | CuO | 0.0003 |
| 7 | Fe ₂ O ₃ | 0.1235 |
| 8 | MgO | 2.2345 |
| 9 | Mn | 0.0955 |
| 10 | Mo | 0.03402 |
| 11 | Ni | 0.0418 |
| 12 | SiO ₂ | 4.3453 |
| 13 | Ta | 0.0004 |
| TOTAL | | 100 |

Table 4.7 shows that Calcium oxide has the highest composition of elements (92%) followed by a far distance of silicon oxide (4.3%) and magnesium oxide (2.2%), copper

oxide (0.0003%) has the lowest amount of elements. Other elements are approximately 1% or far away from 0.5%.

4.1.4 Thermogravimetric Analysis (TGA)

Analysis of Obajana limestone using TGA is shown in Figure 3. It showed the percentage weight loss against temperature for thermal decomposition of Obajana limestone. The figure shows that the decomposition took place between 720°C to 820°C. Thermal decomposition reaction of limestone began at 28.14°C and terminated at 900°C. The rate of weight loss corresponding to the thermal decomposition of calcium carbonate to calcium oxide, increased as temperature increases and reaches a maximum at 820°C. At temperatures above the maximum rate, the rate of weight loss decreased as lesser amounts of calcium carbonate remained in the sample. Eventually the rate became zero because all the calcium carbonate in the sample decomposed to calcium oxide. The onset weight loss is about 2.003%

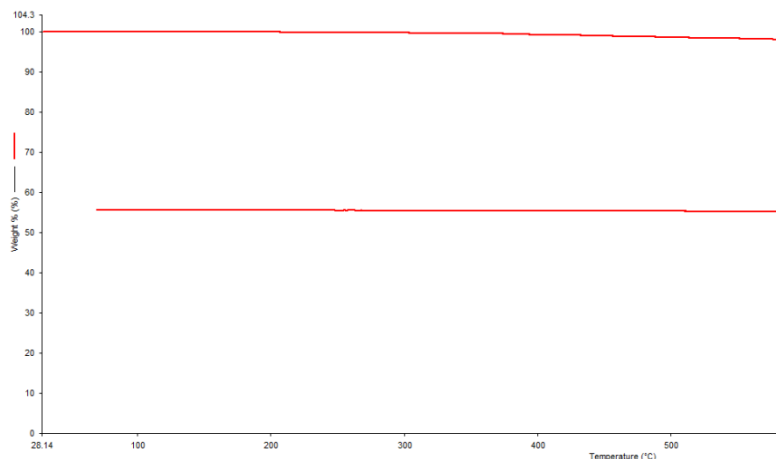


Figure 3: Thermogravimetry of Obajana limestone from 28.14 °C to 900 °C.

4.2 Kinetic Studies of Thermal Decomposition of Obajana Limestone.

4.2.1 Determination of Kinetic parameters

Kinetic parameters were determined by using samples with different particle sizes, against respective temperature values that gives the best correlation coefficient from the thermogravimetric Analysis data of Obajana limestone using the rate of reaction order.

For first order reaction, the following particle sizes were used: 450 μ , 600 μ and 2000 μ for the determination of kinetic parameters.

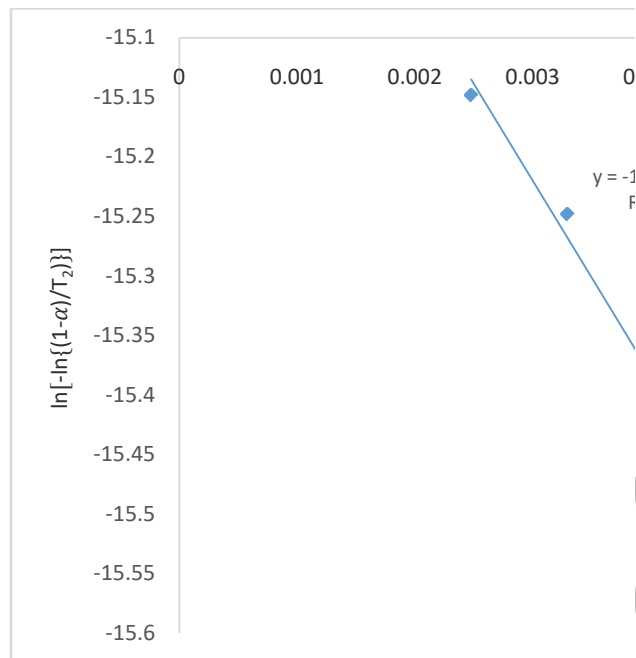


Figure 4: Graph of $\ln[-\ln\{(1-\alpha)/T_2\}]$ against $1/T$ for 450 μ particle size.

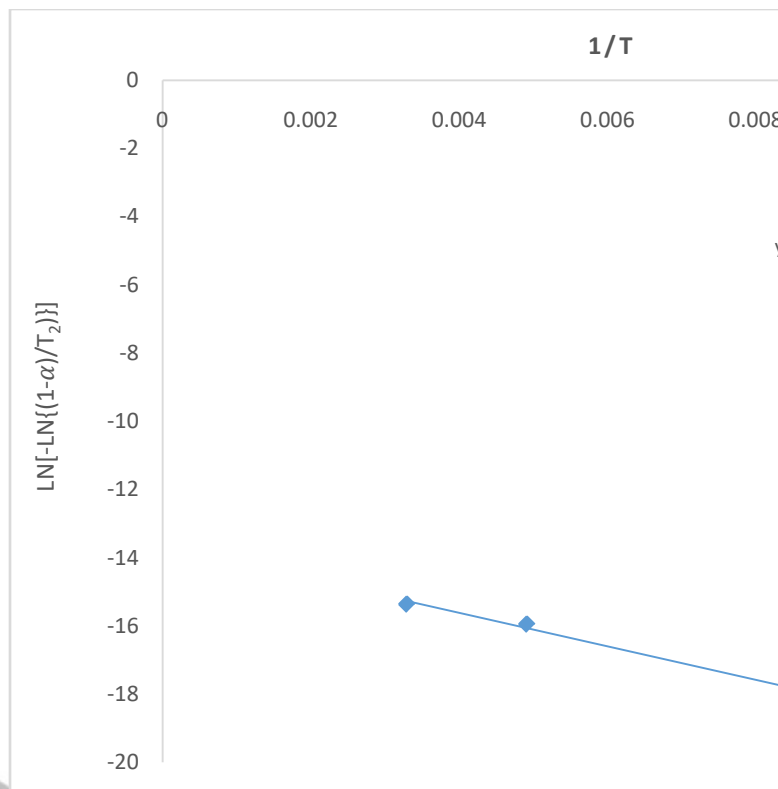


Figure 5: Graph of $\ln[-\ln\{(1-\alpha)/T_2\}]$ against $1/T$ for 600 μ particle size.

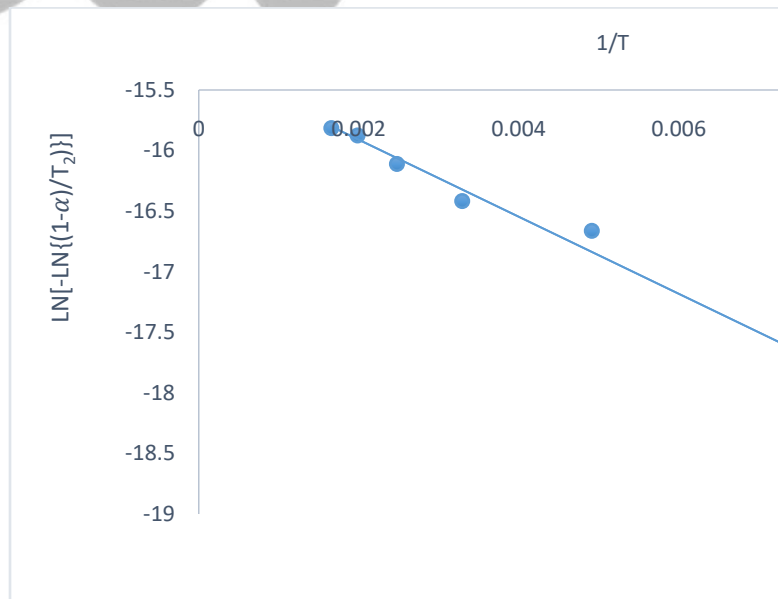


Figure 6: Graph of $\ln[-\ln\{(1-\alpha)/T_2\}]$ against $1/T$ for 2000 μ particle size

Also for second order reaction, the following particle sizes were used: 450 μ , 600 μ and 2000 μ for the determination of kinetic parameters.

4.2.2 Determination of rate order of reaction

According to Samtani et al. (1980), value of $f(\alpha)$ is dependent on types of reaction order which can be decided upon the best fit curved. From the graphs it can be seen that the best fit curved were chosen using the best mathematical model for reaction mechanism. This is represented in Table 4

Table 4: Mathematical Model for Reaction Mechanism.

| Type of order equation | $f(\alpha)$ |
|------------------------|-------------|
| First order | $1-\alpha$ |

Consequently, it can be deduced that the order of reactions used in this research work gave an accurate curve which were assessed

by regression coefficient values (R^2). These are further explained below.

From the graphs of $\ln[-\ln \{(1-\alpha)/T_2\}]$ against $1/T$ for particle sizes of 450 μ , 600 μ and 2000 μ , using first order reactions and based on the plotted curve, it can be deduced that Figure 2 which has a particle size of 450 μ has regression coefficient value of $R^2 = 0.9927$, and for Figure 3 which has a particle size of 600 μ has a regression coefficient of $R^2 = 0.9957$, also Figure 4 which has a particle size of 2000 μ further give the regression coefficient of $R^2 = 0.9902$. Base on the curve plotted, it can also be deduced that from figure 4.5, 4.6 and 4.7, the regression coefficients of R^2 are, 0.9955, 0.9963 and 0.9982 respectively. The values of regression coefficients R^2 from the plots showed that they are close to unity which is deemed to provide the best fit for the calcination of Obajana limestone stone.

4.2.3 Determination of activation energy

E_a.

Activation energy was calculated by using the kinetic constants from the kinetic model equation best fitted from the experimental data. In this research, first and second order kinetic models were used. Based on the curve plotted, activation energy were obtained from each of the slope of the straight line graph. The activation energy are given below.

Table 5: Kinetic Analysis for Particle Size Samples Showing the Activation Energy using First Order Reaction

| S/ No | Parti cle size (μ) | E _A (kJ/mol) | Frequ ency factor (A) | R ² | Res ults |
|-------|--------------------|-------------------------|-----------------------|----------------|----------|
| 1 | 450 | 8.108× | | | |
| | | 10 ³ | 6.45× | 0.99 | |
| | | | 10 ⁸ | 27 | |
| 2 | 600 | 9.807× | | | |
| | | 10 ³ | 8.21× | 0.99 | |
| | | | 10 ⁹ | 57 | |
| 3 | 2000 | 1.059× | | | |
| | | 10 ⁴ | 1.85× | 0.99 | |

10¹⁰ 02

It can be deduced from table 2 and 3 that activation energy decreases with increasing particle size for the first order kinetics model. This result is in conformation with collision theory that the smaller the activation energy the greater activity, which is linked to the kinetics calcination of Obajana limestone. This is further explained by the fact that there is increasing diffusional resistance to the escape of carbon dioxide from the particle interior as the particle size increases. The result is in agreement with that obtained by Halikla et al. (2001)

4.2.4 Determination of Frequency Factor (A)

The pre-exponential factor for this research was also calculated using the kinetic parameters obtained from the slope and intercepts of all the graphs plotted for the particle sizes as shown in Tables 2 and 3.

From Table 2 and Table 3, it can be deduced that as particle sizes increases pre-exponential factor reduces. This is also in agreement with collision theory.

From Table 4 and Table 5 it can be observed that for each of the graphs plotted gave a straight line which is in line with the experimental results of other researches using different limestones. Activation Energies (E_A) and pre-exponential values (A) for the limestone samples were calculated from the slope and intercept of their $\ln[-\ln \{(1-\alpha)/T_2\}]$ vs $1/T$ plots. Also since the activation energy values are all positive it is in agreement with literature collision theory, that it is an endothermic process.

4.2.5 Effects of Particle Size on Calcination of Obajana Limestone:

The particle sizes of limestone also have an effect on calcination processes. Theoretically, for the smaller particle size, low activation energy is required and vice

versa for larger particle size. According to Yan et al, intermediate particle size will have reaction and mass transfer limitations. Also calcination rate is also influenced by the pore diffusion resistance that influences the mass transfer to the pores. It can therefore be observed that from Table 2 and Table 3, activation energy reduces vice versa. This result is in agreement with the result obtained by Yusup et al. (2012).

Conclusion

In this research the study of the kinetics of thermal decomposition of Mfamosing high grade limestone was undertaken using the Coats-Redfern Kinetic Model and the following conclusion was drawn:

- OBAJANA Limestone TGA data fitted into Coats-Redfern Kinetic model.
- The kinetic parameter activation energy increased from 7.398×10^3 kJ/mol to 9.998×10^3 kJ/mol as the

- particle size of the limestone increased from 0.45 mm to 2.0 mm
- The pre-exponential factor and activation energy kinetic parameters obtained are in close agreement with that obtained by Sugiyono (2010).
 - The results of Mfamosing limestone characterization (SEM, ICP-OES, XRD) shows that it has the properties of calcite.

REFERENCE

- Boynton, R.S. (1980). Chemistry and Technology of lime and limestone, 2nd; New York; John Wiley and Son.
- Commander, J.M. (2007). Reactivity of laboratory and industrial lime 85,473-480
- Derringer, G.C. (1994). Balancing act: Optimizing a product properties quality progress 26(6) 51-58
- Gerrand A.J. (1988). Rocks and land form; limestone.London macmillan: 29
- Harrington, E.C. (1965B). The experimental design for quadratic response surface. Biometric 15(2) 611-624
- Jimoh, A. (2001). Chemical Deterioration of Long serving cement Based structure in the Lagos industrial Area. Unpublished M.Engr.Thesis Minna Nigeria federal University of Technology, 54-63

Kilic, O. (2005). comparison of Calcination parameters ph.D, Thesis. Department of mining Engineering institute, Cukurova Uni, 171

Lawall, T.R. (1978). Rock products, 81,82

moropoulo, A. (1998). Historic mortar Technology in crete pp 55-72

Myers, R. H., & Montgomery, D. C. (2002). *Response Surface Methodology*. New York: John Wiley & Sons. Mindrup, F. M., (2011). Optimized Hyperspectral Imagery Anomaly Detection through Robust Parameter Design, Ph.D. Dissertation, Department of the Airforce, NAir University, Ohio, 34-46.

Odigure, J.O.(1995).General Chemical Engineering Technology: Minna Nigeria:Jodigs and Associate

Oates, J.A.H. (1998). lime and limestone Chemistry and Technology production and uses. 169

Ola, S. A. (1977). Limestone Deposits and Small Scale Production of Lime in Nigeria. *Engineering Geology*, 11, 128.

Ortiz, F., Simpson, J. R., Pignatiello, J. J., & Heredia-Langner, A. (2004). A Genetic Algorithm Approach to Multiple-Response Optimization. *Journal of Quality Technology*, 36, 432-450.

R.H. (1985). Borgwardt AIChE J, 31, 103

Soltan, A.M (2011). Impact of limestone microstructure on the calcinations vol 11, 409-416

T.Allen (1997) Particle measurement volume 2 surface are and pore size determination.
Chapman and Hall London 5th edition

© GSJ